Widespread Defects in the Primary Olfactory Pathway Caused by Loss of *Mash1* Function

Richard C. Murray,[1,3] Daniel Navi,[1,3] John Fesenko,[2,3] Arthur D. Lander,[2,3] and Anne L. Calof[1,3]

[1]Department of Anatomy and Neurobiology, [2]Department of Developmental and Cell Biology, and [3]Developmental Biology Center, University of California, Irvine, Irvine, California 92697-2300

MASH1, a basic helix-loop-helix transcription factor, is widely expressed by neuronal progenitors in the CNS and PNS, suggesting that it plays a role in the development of many neural regions. However, in mice lacking a functional *Mash1* gene, major alterations have been reported in only a few neuronal populations; among these is a generalized loss of olfactory receptor neurons of the olfactory epithelium. Here, we use a transgenic reporter mouse line, in which the cell bodies and growing axons of subsets of central and peripheral neurons are marked by expression of a *tau-lacZ* reporter gene (the *Tattler-4* allele), to look both more broadly and deeply at defects in the nervous system of *Mash1*−/− mice. In addition to the expected lack of olfactory receptor neurons in the main olfactory epithelium, developing *Mash1*−/−;*Tattler-4*+/− mice exhibited reductions in neuronal cell number in the vomeronasal organ and in the olfactory bulb; the morphology of the rostral migratory stream, which gives rise to olfactory bulb interneurons, was also abnormal. Further examination of cell proliferation, cell death, and cell type-specific markers in *Mash1*−/− animals uncovered parallels between the main olfactory epithelium and the vomeronasal organ in the regulation of sensory neuron development. Interestingly, this analysis also revealed that, in the olfactory epithelium of *Mash1*−/− animals, there is an overproduction of proliferating cells that co-express markers of both neuronal progenitors and supporting cells. This finding suggests that olfactory receptor neurons and olfactory epithelium supporting cells may share a common progenitor, and that expression of *Mash1* may be an important factor in determining whether these progenitors ultimately generate neurons or glia.

Key words: **bHLH transcription factor; olfactory epithelium; olfactory receptor neuron; transgenic mouse; olfactory bulb; rostral migratory stream; subventricular zone; vomeronasal organ; neural progenitor; lineage; supporting cell; granule cell**

Introduction

Basic helix-loop-helix (bHLH) transcription factors appear to play a conserved role in determining neuronal fate during development (Brunet and Ghysen, 1999; Guillemot, 1999). In *Drosophila*, proneural genes such as *achaete*, *scute*, and *atonal* instruct neuronal fate determination (Jan and Jan, 1994), and at least some homologs of these genes play analogous roles in vertebrates. For example, loss of function studies in mice have shown that *Mash1*, *Ngn1*, and *Ngn2* are required for the development of specific subsets of neurons (Guillemot et al., 1993; Fode et al., 1998; Ma et al., 1998).

Mash1, a homolog of *achaete* and *scute*, is expressed by neuronal progenitors in the developing PNS and CNS. In the CNS, *Mash1* is expressed in the developing telencephalon, including ventricular zone (VZ) of the developing olfactory bulb (OB) and ganglionic eminences, diencephalon, midbrain, spinal cord, and retina (Guillemot and Joyner, 1993; Ma et al., 1997; Horton et al., 1999). *Mash1* is also expressed in the PNS, including the olfactory epithelium (OE) and the sympathetic, parasympathetic, and enteric nervous systems (Guillemot and Joyner, 1993; Gordon et al., 1995; Blaugrund et al., 1996; Ma et al., 1997). Although this widespread expression suggests that *Mash1* plays a role in the development of many neural regions, the initial analysis of gene-targeted *Mash1*−/− mice detected deficits only in olfactory receptor neurons (ORNs) and neurons of the autonomic nervous system (Guillemot et al., 1993). Subsequent studies demonstrated additional and more subtle roles for *Mash1*, often acting in concert with other transcriptional regulators, in regulating cell fate and neuronal differentiation in various CNS regions (Casarosa et al., 1999; Horton et al., 1999; Torii et al., 1999; Tomita et al., 2000; Hatakeyama et al., 2001; Marquardt et al., 2001; Nieto et al., 2001). These findings, and the discovery of thalamocortical axon pathfinding defects resulting from loss of *Mash1* (Tuttle et al., 1999), suggest that other neural deficits are likely to be present in *Mash1*−/− animals.

To look systematically for additional phenotypes in *Mash1*−/− animals, as well as other neurodevelopmental mutants, we developed a transgenic mouse line (Tattler-4) that allows rapid visualization of subsets of neurons and their axons during development. Tattler-4 mice were generated using a promoter fragment from the *Tα1 α-tubulin* gene to express a *tau-lacZ* fusion gene. The transgene is expressed in cell bodies and axons of subsets of PNS and CNS neurons during terminal neuronal differentiation and initial axon outgrowth. By breeding the *Mash1* null allele onto Tattler-4 and examining the primary olfactory pathway with β-galactosidase histochemistry, we were able to identify abnormalities in *Mash1*−/− animals not only in OE, but also in the vomeronasal organ (VNO), OB, and rostral

Received May 13, 2002; revised Dec. 11, 2002; accepted Dec. 12, 2002.

This work was supported by National Institutes of Health Grants DC03583 to A.L.C., NS26862 to A.D.L., HD38761 to A.D.L. and A.L.C., and the March of Dimes Birth Defects Foundation (FY00-660 to A.L.C.). We thank Carl Lagenaur for 12F8 anti-PSA-NCAM monoclonal antibody, Tom Curran for *reelin* probe, and Shimako Kawauchi for help with *in situs*.

Correspondence should be addressed to Anne L. Calof, Department of Anatomy and Neurobiology, 364 Med Surge II, University of California, Irvine, Irvine, CA 92697-1275. E-mail: alcalof@uci.edu.

 0270-6474/03/231769-12$15.00/0

migratory stream (RMS), a structure containing neural progenitors that give rise to OB interneurons. Analysis of gene expression in the developing OE and VNO of *Mash1*−/− animals uncovered parallels in genetic regulation of sensory neuron development between these two tissues and provided clues that ORNs and OE supporting cells share a common progenitor.

Materials and Methods

Transgenic mice. The *Tα1*:*tau-lacZ* transgene was generated by ligating a 5.5 kb *Xho*I/*Spe*I fragment containing the *tau-lacZ* fusion and SV40 splice site and poly(A) addition sequence (Callahan and Thomas, 1994) downstream of a 1.1 kb *Bss*HII/*Xba*I fragment of the *Tα1 α-tubulin* promoter (Gloster et al., 1994) (see Fig. 1*A*). To generate transgenic mice, the *Tα1*:*tau-lacZ* construct was linearized with *Asc*I/*Pme*I and injected into pronuclei of fertilized mouse ova (CB6 F2) using standard techniques (Hogan, 1994) in the University of California, Irvine, Transgenic Mouse Facility. Transgenic offspring were identified by PCR of tail DNA and bred against CD-1 mice (Charles River Laboratories, Wilmington, MA) to generate four independent transgenic mouse lines, named Tα1-tubulin tau-lacZ expressing reporter (Tattler) 1–4. Tattler-4 mice, used in this study, were bred for more than eight generations on a CD-1 background. *Mash1*+/– mice were a generous gift from F. Guillemot (IGBMC, Strasbourg, France) (Guillemot et al., 1993) and were maintained on a CD-1 background, where the OE phenotype is fully penetrant (Cau et al., 1997; this study). *Tattler-4*+/+;*Mash1*+/– animals were mated with *Mash1*+/– females to generate *Tattler-4*+/–;*Mash1*+/+ and *Tattler-4*+/–;*Mash1*−/− littermate embryos for analysis.

Genotype was determined by PCR (30 cycles, annealing temperature 58°C) of tail or yolk sac DNA using oligonucelotide primers (Invitrogen, San Diego, CA) specific for *lacZ* for Tattler-4 animals or for *Mash1* and *neo* to distinguish *Mash1*+/+, +/−, −/− genotypes (*lacZ*, GenBank accession number V00296; LacZ-Forward, 5′-TGATGAAAGCTGGCTACAT-3′; LacZ-Reverse, 5′-ACCACCGCACGATAGAGATT-3′; *Mash1*, GenBank U68534; Mash1-Forward, 5′-CCAACTGGTTCTGAGGAC-3′; Mash1-Reverse, 5′-CCCATTTGACGTAGTTGG-3′; *neo*, GenBank U43611; Neo-Forward, 5′-GATCTCCTGTCATCTCACCT-3′; Neo-Reverse, 5′-ATGGGTCACGACGAGATCCT-3′).

In situ *hybridization, immunohistochemistry, and terminal deoxynucleotidyl transferase-mediated biotinylated UTP nick end labeling staining.* One hour before they were killed, timed-pregnant female mice were injected intraperitoneally with 50 μg/gm body weight of 5-bromo-2′-deoxyuridine (BrdU) (5 mg/ml in 0.9% saline, 0.007N NaOH). Pregnant dams were killed, and embryos were dissected and fixed overnight in 4% paraformaldehyde in 0.02 M $NaPO_4$, 0.15 M NaCl, pH 7.5. Embryos were washed in PBS, cryoprotected in 30% sucrose/PBS, and sectioned at 12 or 20 μM on a cryostat. Sections were collected on Superfrost/Plus slides (Fisher Scientific, Houston, TX) and stored at −80°C until use. For staging of embryos, 12:00 P.M. on the day a vaginal plug was detected was designated embryonic day (E) 0.5.

For *in situ* hybridization, sections were fixed onto slides in 4% paraformaldehyde/PBS, washed in PBS, incubated with proteinase K (25 μg/ml, 10–15 min), refixed in 4% paraformaldehyde/PBS, acetylated (0.25% acetic anhydride in 0.1 M triethanolamine, pH 8.0), and hybridized at 60°C in 50% formamide, 5× SSC, 300 μg/ml Yeast tRNA, 100 μg/ml heparin, 1× Denhardt's, 0.1% Tween 20, 0.1% CHAPS, and 5 mM EDTA containing 100 ng/ml probe. Unbound probe was removed by washing (0.2× SSC, 60°C), and probes were detected using alkaline phosphatase-conjugated sheep anti-DIG antibodies (1:2000) (Roche Molecular Biochemicals, Indianapolis, IN) and visualized using 5-bromo-4-chloro-3-indolyl-phosphate (BCIP)/4-nitroblue tetrazolium chloride (NBT) as substrate. Slides were dehydrated and mounted in Pro-Texx (Lerner Laboratories, Pittsburgh, PA) before viewing. The probes that were used were as follows: 375 bp fragment of mouse *Mash1* coding region, 2.0 kb fragment of mouse *Mash1* gene including coding region and 3′UTR [Clone 1 in Guillemot and Joyner (1993)], 1.2 kb fragment of rat *ngn1* gene (Ma et al., 1996), 391 bp fragment of mouse *Ncam* coding region (Barthels et al., 1987), 1.7 kb fragment of the mouse *Trp2* coding region (Vannier et al., 1999), and 155 bp fragment of the mouse *reelin* coding region (D'Arcangelo et al., 1995). The *steel* probe consisted of an 879 bp fragment of the mouse *steel* coding region and 3′UTR (GenBank M57647) (bp 386–1265), generated by RT-PCR of mouse E12.5 head total RNA. The PCR product was cloned into the pCR2.1 vector (Invitrogen), and its identity was confirmed by sequencing. The *Gad67* probe consisted of an 867 bp fragment of the mouse *Gad67* 3′UTR (GenBank NM008077) (bp 1987–2854), generated by RT-PCR of mouse P1 brain total RNA. The PCR product was cloned into pBluescript (Stratagene, La Jolla, CA), and its identity was confirmed by sequencing.

For BrdU immunostaining, sections were permeabilized in 0.1% Triton X-100 in PBS (30 min, room temperature), treated with 2N HCl (1 hr, 37°C), neutralized in HBSS (Invitrogen), blocked in 0.1% Triton X-100, 10% bovine calf serum (BCS) (HyClone, Logan, UT) in PBS, incubated with anti-BrdU antibody (clone BU1/75) (1:1000 in 10% BCS in PBS; overnight, 4°C) (Harlan Sera-Lab, Sussex, UK), and visualized with Texas Red-conjugated goat anti-rat IgG (1:50) (Jackson ImmunoResearch, West Grove, PA). Immunostaining with monoclonal anti-neuron-specific nuclear protein (NeuN) (1:500 dilution) (Chemicon, Temecula, CA) was performed in the same manner but without acid treatment, and primary antibody was detected using Texas Red-conjugated goat anti-mouse IgG1 (1:50) (Southern Biotechnology, Birmingham, AL). For immunostaining with 12F8 monoclonal anti-polysialic acid (PSA) neural cell adhesion molecule (NCAM) (Carl Lagenaur, University of Pittsburgh), hybridoma supernatant was applied overnight at 4°C and detected using Texas Red-conjugated goat anti-rat IgM (1:50) (Jackson ImmunoResearch).

Terminal deoxynucleotidyl transferase-mediated biotinylated UTP nick end labeling (TUNEL) staining to detect DNA fragmentation *in situ* was performed as described previously (Holcomb et al., 1995), using Texas Red-conjugated NeutrAvidin (Molecular Probes, Eugene, OR) to detect incorporated Biotin-16-dUTP (Roche Molecular Biochemicals).

β-galactosidase histochemistry. E13.5 whole-mount staining was performed as described previously (Murray et al., 2000). For older embryos, tissues were dissected and fixed by immersion in 2 mM $MgCl_2$, 4% paraformaldehyde in 0.02 M $NaPO_4$, 0.15 M NaCl, pH 7.5, for 2–4 hr at room temperature, washed three times 5 min in 2 mM $MgCl_2$ in PBS at room temperature, cryoprotected in 30% sucrose, 2 mM $MgCl_2$ in PBS, and sectioned at 30 μm on a cryostat. Sections were collected on gelatin-coated slides, postfixed in 2 mM $MgCl_2$, 0.5% glutaraldehyde, in PBS for 15 min, and permeabilized in 2 mM $MgCl_2$, 0.1% Triton X-100, 0.01% deoxycholate, in PBS for 10 min. Sections were stained overnight in 1 mg/ml 5-bromo-4-chloro-3-indolyl β-D-galactopyranoside (X-gal), 5 mM $K_3Fe(CN)_6$, 5 mM $K_4Fe(CN)_6$, 2 mM $MgCl_2$, 0.1% Triton X-100, 0.01% deoxycholate, in PBS at 37°C, and then dehydrated and mounted in Pro-Texx.

Results

Subsets of neurons in the PNS and CNS are marked in Tattler-4 transgenic mice

To study the connectivity of developing neuronal populations in the embryonic mouse nervous system, we generated transgenic mice that express an axon-targeted reporter gene in differentiating neurons. A 1.1 kb fragment of 5′ regulatory sequence from the *Tα1 tubulin* gene was used to drive expression of a reporter construct (*tau-lacZ*), which consisted of a fragment of the bovine gene encoding the microtubule-associated protein, tau, fused to the bacterial β-galactosidase gene (*lacZ*) (Callahan and Thomas, 1994; Gloster et al., 1994). The resulting construct (*Tα1:tau-lacZ*) (Fig. 1*A*) was used to generate four independent transgenic mouse lines, which were named *Tα1-tubulin tau-lacZ* expressing reporter (Tattler) 1–4. The Tattler-4 strain had the most extensive pattern of expression and was chosen for further analysis.

To reveal the overall expression pattern of *Tα1:tau-lacZ* expression in Tattler-4 mice, transgenic embryos were fixed and stained with X-gal as whole mounts at day 13.5 of gestation (E13.5). As shown in Figure 1, *B* and *C*, X-gal staining was specific

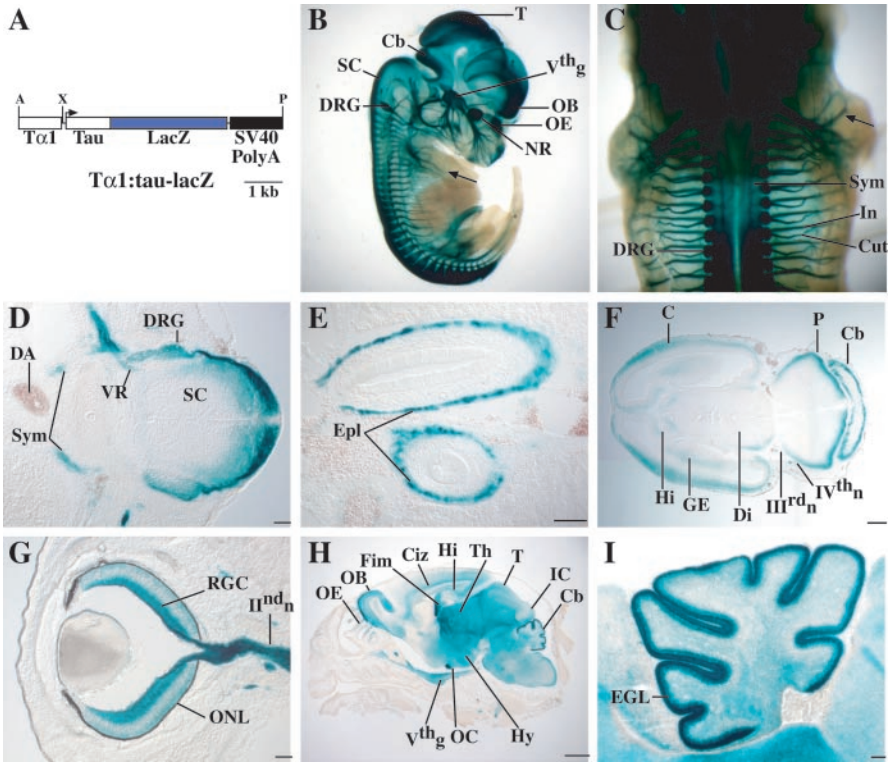

Figure 1. *A*, Diagram of the *Tα1:tau-lacZ* transgenic construct used to generate Tattler-4 mice. The *tau-lacZ* reporter fusion is expressed under the control of the *Tα1 α-tubulin* promoter. A polyadenylation signal from SV40 is included in the construct. *A*, *AscI*; *X*, *XhoI*; *P*, *PmeI*. *B-I*, *Tα1:tau-lacZ* expression in Tattler-4 transgenic mice. Expression was visualized by X-gal staining, as detailed in Materials and Methods. *B*, Sagittal view of E13.5 Tattler-4 transgenic embryo stained with X-gal. Staining is present in the neural retina (*NR*), olfactory epithelium (*OE*), olfactory bulb (*OB*), tectum (*T*), cerebellum (*Cb*), dorsal spinal cord (*SC*), trigeminal ganglion ($V^{th}g$), and dorsal root ganglia (*DRG*). Sensory nerves in the limb (*arrow*) are also stained. *C*, Dorsal view of E13.5 embryo. The sympathetic chain (*Sym*) underlying the spinal cord, dorsal root ganglia (*DRG*), cutaneous (*Cut*), and intercostal (*In*) spinal nerves are stained. *D*, Transverse section through the spinal cord of an E13.5 embryo. Staining is present in the dorsal spinal cord (*SC*) and dorsal root ganglia (*DRG*) as well as in the sympathetic chain (*Sym*). Staining in the ventral root (*VR*) likely represents preganglionic sympathetic axons, because the ventral horn motor neurons are not stained. The dorsal aorta (*DA*) is labeled for reference (dorsal is at the *right*). *E*, Horizontal section through the abdomen of an E13.5 embryo. Staining is present in the enteric plexus (*Epl*) of the developing gut. *F*, Horizontal section through the head of an E13.5 embryo stained in whole mount. Staining is present at the margin of the cerebral cortex (*C*), pons (*P*), cerebellum (*Cb*), diencephalon (*Di*), ganglionic eminence (*GE*), and hippocampus (*Hi*). The oculomotor ($III^{rd}n$) and trochlear ($IV^{th}n$) cranial nerves are also stained. *G*, Horizontal section through the eye of an E16.5 embryo. Prominent staining is present in the retinal ganglion cells (*RGC*) and their axons in the optic nerve ($II^{nd}n$). Some staining in the developing outer nuclear layer (*ONL*) is also apparent. *H*, Parasagittal section through the head of a P0 animal. Staining is present in the *OE*, *OB*, intermediate zone of the cerebral cortex (*Ciz*), hippocampus (*Hi*), fimbria (*Fim*), thalamus (*Th*), optic chiasm (*OC*), hypothalamus (*Hy*), tectum (*T*), inferior colliculus (*IC*), cerebellum (*Cb*), and trigeminal ganglion ($V^{th}g$). *I*, Parasagittal section through the cerebellum of a P0 Tattler-4 mouse. Staining is present in cells of the external granule layer (*EGL*). Scale bars: *D*, *E*, *G*, *I*, 100 μm; *F*, 300 μm; *H*, 1 mm.

to neurons and was present in both neuronal cell bodies and axons in a subset of neural structures in both the CNS and PNS. In the CNS, prominent staining was observed in the retina, olfactory bulbs, telencephalon, diencephalon, midbrain, hindbrain, and spinal cord (Fig. 1*B*). In addition, cranial sensory ganglia and nerves, including the trigeminal, oculomotor, and trochlear nerves, were labeled by X-gal staining (Fig. 1*B*). In the PNS, expression was seen in the dorsal root ganglia and cutaneous and intercostal spinal nerves (Fig. 1*C*). Sections made from E13.5 X-gal-stained whole mounts revealed that both sympathetic nerve fibers (Fig. 1*D*) and the enteric plexus were labeled (Fig. 1*E*). These sections also revealed that staining of the dorsal spinal cord could be attributed to labeled fibers of the dorsal root entry zone; developing motoneurons and interneurons were not labeled (Fig. 1*D*). Brain sections from E13.5 whole mounts showed X-gal staining at the margins of structures such as cortex, diencephalon, ganglionic eminence, and pons, but not in the respective ventricular zones (Fig. 1*F*). This suggests that the transgene is expressed primarily by postmitotic neurons rather than neuronal progenitors and is consistent with what is known about time of onset of terminal neuronal differentiation in these regions (Angevine, 1970; Pierce, 1973; Nornes and Carry, 1978; McConnell, 1981). Because previous studies have shown that the *Tα1 tubulin* promoter fragment that we used drives reporter gene expression in embryonic neurons at the time of terminal differentiation and initial axon outgrowth (Gloster et al., 1994, 1999), these observations suggested that X-gal staining in Tattler-4 mice reveals the axons and, to a lesser extent, cell bodies, of newly differentiating neurons.

Examination of Tattler-4 embryos at older ages revealed high levels of reporter expression in distinct subsets of neurons in different regions of the CNS. For example, in the developing neural retina at E16.5, retinal ganglion cells and their axons were darkly stained; light staining was also observed in cells of the developing outer nuclear layer (ONL) (Fig. 1*G*). At postnatal day (P) 0, staining could be seen in a subset of cells and their axons in the cerebral cortex, hippocampus, fimbria, and striatum; fiber tracts in the diencephalon and midbrain were also labeled (Fig. 1*H*). Especially prominent staining was observed in the ORNs of the OE and associated olfactory nerve, the glomeruli and mitral/tufted cell layer of the olfactory bulb; and cells of the external granule layer, but not Purkinje cells, in the cerebellum (Fig. 1*H*,*I*). Expression of the *Tα1:tau-lacZ* transgene in only a subset of CNS and PNS neurons can likely be attributed to sensitivity of the *Tα1-tubulin* promoter fragment to the site of transgene integration; other investigators have generated transgenic lines using this promoter to drive a nuclear *lacZ* reporter gene, and the subset of expressing neurons varied in different lines (Gloster et al., 1994). Because expression of *Tα1:tau-lacZ* by specific populations of neurons in Tattler-4 mice is a stable characteristic of all mice in this transgenic line, it provides a useful tool for selectively examining the behavior of these cells as development of the nervous system proceeds.

Tα1:tau-lacZ reporter gene expression reveals unexpected changes in the olfactory bulb and rostral migratory stream of *Mash1*−/− mice

Because the *Tα1:tau-lacZ* reporter gene is expressed strongly in several structures of the primary olfactory pathway in Tattler-4 mice, we used these animals to help us examine development of this pathway in animals in which the gene encoding the basic helix-loop-helix transcription factor, MASH1, has been dis-

rupted by homologous recombination. *Mash1*−/− mice die at birth and have been demonstrated previously to have a profound reduction in the number of ORNs in the OE lining the nasal cavity (Guillemot et al., 1993). Because *Mash1* is known to be expressed in the developing telencephalon, including the OB (Guillemot and Joyner, 1993; Sommer et al., 1996), we hypothesized that other defects might be present in the primary olfactory pathway of *Mash1*−/− mice. To test this possibility, we bred the *Mash1* knock-out allele onto the Tattler-4 background and compared olfactory structures in *Mash1*−/− animals and their wild-type littermates.

We first examined mice around the time of birth (E18.5/P0), because *Mash1*−/− animals only survive to this age. At E18.5, X-gal staining of *Mash1*+/+;*Tattler-4*+/− mice revealed expression of *tau-lacZ* in ORN cell bodies within the OE and in ORN axons projecting to the OB (Fig. 2*A*). Also labeled by X-gal staining were cells in the mitral/tufted cell layer of the OB; these are the cell types onto which ORNs synapse. However, cells in the developing OB granular layer, which contains primarily granule cell interneurons, were not stained (Fig. 2*A*) (Farbman, 1992). In contrast to the situation in wild-type embryos, the OE of *Mash1*−/−;*Tattler-4*+/− embryos was devoid of X-gal staining and was much thinner than normal, and ORN axons were virtually absent (Fig. 2*B*). Thus, the *Tattler-4* allele clearly revealed the deficit in ORN development known to occur in the absence of *Mash1* function.

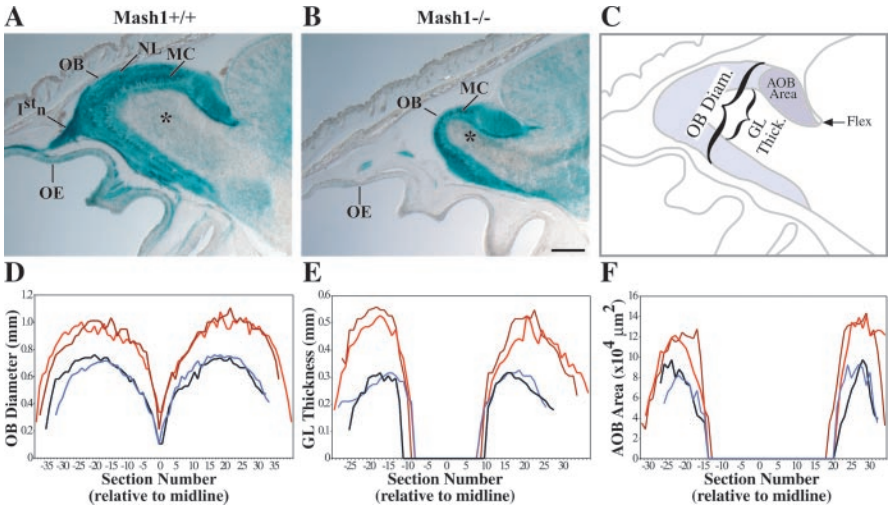

Figure 2. Alterations in the OE and OB of *Mash1*−/− mice. *A*, *B*, E18.5 littermate embryos heterozygous for the *Tattler-4* reporter allele and *Mash1*+/+ (*A*) or *Mash1*−/− (*B*) were sectioned at 30 μm in the sagittal plane and stained with X-gal. Anterior is on the *left*; dorsal is at the *top*. The olfactory epithelium (*OE*), mitral/tufted cell layer (*MC*), outer nerve layer (*NL*), olfactory nerve (*I^st n*), and granular layer (*asterisk*) are shown. Scale bar, 300 μm. *C*, Diagram to illustrate the measurements taken to quantify changes in OB and AOB size. OB diameter and granular layer (*GL*) thickness were measured in the plane perpendicular to the cribriform plate, at the point midway between the anterior tip of the OB and the flexure at the junction of the anterior border of the cerebral cortex and the dorsal surface of the OB (*labeled brackets*). OB diameter was measured as the distance between the dorsal and ventral surfaces of the OB; GL thickness was measured as the distance across the unstained granular layer in X-gal-stained tissue. AOB area (*light blue shading*) was measured using NIH Image 1.61. *D*, Decreased OB diameter in *Mash1*−/− embryos. To quantify changes in the size of the OB, serial 30-μm-thick sagittal sections through the entire extent of both OBs were measured in two *Mash1*−/−;*Tattler-4*+/− and two *Mash1*+/+;*Tattler-4*+/− animals at E18.5. A total of 67–80 measurements were taken per animal and plotted relative to the distance of the measured section from the midline. *Mash1*−/− embryos (*blue lines*) and wild-type embryos (*red lines*) are shown. *E*, Decreased GL thickness in *Mash1*−/− embryos. A total of 32–50 measurements were taken per animal and plotted as in *D*. *F*, Reduced AOB area in *Mash1*−/− embryos. A total of 24–35 measurements were taken per animal and plotted as in *D*.

X-gal staining of *Mash1*−/−;*Tattler-4*+/− embryos also revealed that the OBs of these animals were reduced in size compared with their wild-type littermates (Fig. 2*B*). In addition to a size reduction caused by absence of the olfactory nerve layer of the bulb (expected because of the lack of ingrowing ORN axons), the granular layer of the OB appeared to be greatly reduced in size in *Mash1*−/−;*Tattler-4*+/− embryos relative to *Mash1*+/+;*Tattler-4*+/− littermates (Fig. 2*A*,*B*, *asterisks*). Moreover, the accessory olfactory bulb (AOB) (the synaptic target of vomeronasal sensory neurons) (Halpern, 1987) also appeared to be smaller in *Mash1*−/−;*Tattler-4*+/− embryos.

To quantify these changes, we measured the diameter of the OB, the thickness of the granular layer (the cell layer containing developing granule interneurons) within the OB, and the area of the AOB through the entire extent of both bulbs in two *Mash1*−/−;*Tattler-4*+/− and two *Mash1*+/+;*Tattler-4*+/− littermate embryos (Fig. 2*C*). The data, shown in Figure 2*D-F*, demonstrate clear reductions in size of both the OB and the AOB in *Mash1* mutant animals. The diameter of the OB of *Mash1*−/−;*Tattler-4*+/− animals was reduced by 27% relative to their *Mash1*+/+;*Tattler-4*+/− littermates, and the thickness of the granular layer was reduced by 45% in *Mash1* mutants relative to wild-type littermates. The average area of the AOB also showed a large reduction, being decreased by 30% in *Mash1*−/−;*Tattler-4*+/− animals relative to their *Mash1*+/+;*Tattler-4*+/− littermates. To confirm that the reduction in the size of the OB in *Mash1*−/−;*Tattler-4*+/− animals is not caused by the *Tattler-4* allele, the diameter of the OB was measured in *Mash1*−/− animals and their wild-type littermates maintained on a CD-1 background. A similar decrease in OB diameter (29%) in *Mash1*−/− animals relative to wild types was observed (wild type, 0.91 ± 0.03 mm; *Mash1*−/−, 0.65 ± 0.01 mm, for three animals of each genotype; more than eight sections measured per animal).

Granule cell interneurons of the OB originate in the subventricular zone of the lateral ventricles and migrate to the OB in a structure known as the RMS (Luskin, 1993; Lois and Alvarez-Buylla, 1994). The *Tattler-4* reporter allele is expressed by cells of the RMS, allowing this structure to be visualized easily in X-gal-stained sections of normal and *Mash1*−/− animals on the *Tattler-4* background. In sagittal sections through the brains of wild-type animals at E18.5, the RMS could be seen as a stream of cells, many of which were stained with X-gal, extending from the anterior limit of the lateral ventricle to the caudal boundary of the OB (Fig. 3*A*). Interestingly, in *Mash1*−/−;*Tattler-4*+/− embryos, the RMS was present, but its shape was different, being noticeably thicker in *Mash1*−/−;*Tattler-4*+/− animals than in their wild-type littermates (Fig. 3*B*). Moreover, the density of X-gal-stained cells in the RMS of *Mash1*−/−;*Tattler-4*+/− animals was consistently greater than what was observed in wild types (Fig. 3, compare *C*, *D*). Because induced absence of the highly sialylated form of NCAM is associated with similar morphological changes in the RMS, as well as reduced OB size (Bruses and Rutishauser, 2001), we used a monoclonal antibody specific for the PSA moieties on the "embryonic" form of NCAM to stain sections through the RMS in E17.5 *Mash1*−/− and *Mash1*+/+ littermates (Chung et al., 1991). As shown in Figure 3*E*, in wild-

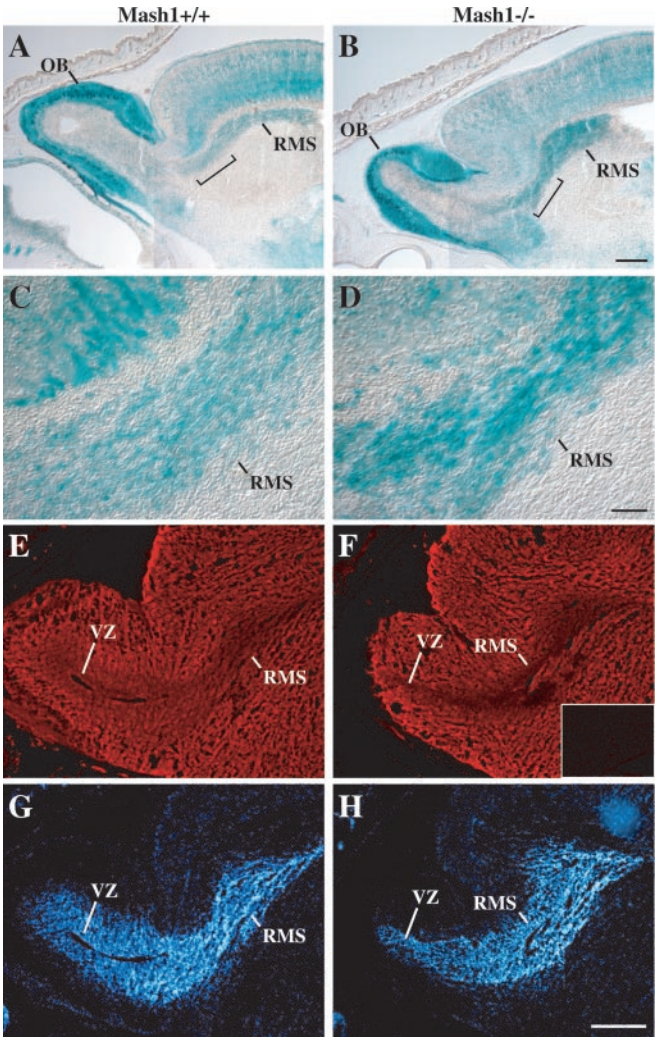

Figure 3. Comparison of the rostral migratory stream in *Mash1*−/− and *Mash1*+/+ embryos. *A–D*, Thirty micrometer sagittal sections through the head of an E18.5 *Mash1*+/+; *Tattler-4*+/− embryo (*A*, *C*) and a *Mash1*−/−;*Tattler-4*+/− littermate (*B*, *D*) stained with X-gal. *C*, *D*, Higher power images of the regions *bracketed* in *A* and *B*. *E–H*, Twelve micrometer sagittal sections through the head of an E17.5 *Mash1*+/+ embryo (*E*, *G*) and a *Mash1*−/− littermate (*F*, *H*) processed for PSA-NCAM immunostaining (monoclonal anti-PSA-NCAM 12F8) (Chung et al., 1991) (*E*, *F*) or nuclear DNA staining (bisbenzimide H 33258 counterstain of same sections) (*G*, *H*). *Inset* in *F* shows a negative control (no primary antibody) section of forebrain, including a portion of the lateral ventricle, for comparison. Rostral migratory stream (*RMS*) and ventricular zone (*VZ*) are shown. Scale bars: (in *B*) *A*, *B*, 250 μm; (in *D*) *C*, *D*, 50 μm; (in *H*) *E–H*, 300 μm.

type embryos, essentially the entire forebrain and OB are stained with the 12F8 monoclonal anti-PSA-NCAM. The cell-dense RMS and ventricular zone of the OB (visualized with a nuclear stain in Fig. 3*G*) are also immunopositive for PSA-NCAM, although as described previously, staining is less intense than in the surrounding brain regions (Chung et al., 1991). In *Mash1*−/− embryos, the level of anti-PSA-NCAM immunoreactivity observed in the RMS and OB ventricular zone was similar to that in wild types (Fig. 3*F*,*H*). Thus, there is no obvious change in expression of PSA-NCAM in the absence of *Mash1* function.

Many of the neuronal cells migrating in the RMS are known to be progenitors of OB granule cells; these progenitors are unusual in that they express markers characteristic of differentiated neurons (e.g., neuronal tubulins) while still continuing to proliferate (Luskin, 1998). Granule cell progenitors follow a stereotyped migratory route into the OB: they first migrate tangentially into the OB along the ventricular zone and then disperse radially into the surrounding granular layer (Alvarez-Buylla, 1997; Luskin, 1998). To determine whether this pattern of cell migration is disrupted in *Mash1*−/− animals, E17.5 embryos were given a pulse of BrdU to label migratory progenitors and then killed 1 hr later, and their brains were fixed and processed for BrdU immunoreactivity. As shown in Figure 4, *A* and *B*, the patterns of dispersal of BrdU-labeled cells were very different in *Mash1*−/− embryos and their wild-type littermates. In wild-type embryos, many BrdU+ cells could be seen outside of the ventricular zone, dispersed within the granular layer (Fig. 4*A*). In contrast, BrdU+ cells in the OB of *Mash1*−/− animals were restricted to the ventricular zone, which itself appeared thinner than that of wild types (Fig. 4*B*). These observations were confirmed by counting the number of BrdU-labeled cells in three concentric bands surrounding the ventricle of the OB in these sections (Fig. 4*C*). In *Mash1*+/+ embryos, many cells were found to have migrated radially out of the ventricular zone and into the surrounding granular layer (i.e., out of Band I into Bands II and III), whereas in *Mash1*−/− animals, virtually all BrdU-positive cells in the OB were found within the ventricular zone (Band I). This observation suggested that, in *Mash1*−/− animals, granule cell progenitors may fail to migrate out of the RMS and into the developing granular layer of the OB, resulting in a deficit in differentiated granule cells and a marked reduction in OB size.

To investigate this idea, we performed *in situ* hybridization experiments to determine whether, in *Mash1*−/− animals, the BrdU+ cells apparently "trapped" in the RMS and VZ of the OB are progenitors that would normally express the *Mash1* gene. To do this, we took advantage of the fact that the noncoding second exon of the *Mash1* gene was still present in the targeting vector used to generate the *Mash1*−/− animals that were used in our study (Guillemot et al., 1993). It has been shown previously that transcripts continue to be made from the disrupted *Mash1* allele in CNS neural progenitors present in *Mash1*−/− animals (Horton et al., 1999). This finding suggested that a probe that includes the *Mash1* 3′UTR could be used to identify cells that express *Mash1* transcripts in *Mash1*−/− animals, as well as normal *Mash1*-expressing progenitors in wild types. When we performed *in situ* hybridization experiments using such a probe (3′ *Mash1* probe), we found that the pattern of hybridization in the RMS/VZ and developing granular layer of the OB showed close correspondence to the pattern of anti-BrdU immunoreactivity (Fig. 4*D*,*E*). Cells positive for the 3′ *Mash1* probe were present in the VZ and dispersed within the developing OB granular layer in wild-type animals (Fig. 4*D*), whereas they were restricted to the VZ in the OB of *Mash1*−/− animals (Fig. 4*E*). This finding suggested that the cells to which the *Mash1* 3′ probe hybridized are neuronal progenitors that would normally express *Mash1* and migrate out of the RMS/VZ and into the granular layer of the OB. However, in *Mash1*−/− animals, these cells are unable to migrate and contribute to OB development, apparently because of a defect resulting from lack of *Mash1* function.

To further investigate the role of *Mash1* in the development of intrinsic OB neuronal cell types, we performed *in situ* hybridization experiments using specific markers to compare the relative sizes of differentiated OB cell populations in *Mash1*−/− animals and their wild-type littermates. Differentiated granule cells were detected using a monoclonal antibody to the neuronal nuclear marker NeuN (Mullen et al., 1992) and a cRNA probe for *Gad67* (Bulfone et al., 1998), whereas OB mitral cells were identified using a probe for *Reelin* (D'Arcangelo et al., 1995). As shown in

Figure 4, the number of NeuN+ and *Gad67*+ cells was drastically reduced in the granular layer of *Mash1*−/− OB (Fig. 4*I*,*J*) compared with wild type (Fig. 4*F*,*G*), indicating that differentiated granule cells are greatly reduced in number in *Mash1*−/− OB. In contrast, there was no apparent decrease in the number of cells expressing the mitral cell marker *Reelin* in *Mash1*−/− OB (Fig. 4, compare *H*, *K*).

Together, these data indicate that in *Mash1*−/− animals, OB granule cell progenitors appear to be generated but are unable to migrate out of the RMS and VZ into the developing granular layer, resulting in a dramatic decrease in granule cell number and a marked reduction in OB size.

Mash1 is required for sensory neuron development in the vomeronasal organ

Although detection of most odors is mediated by ORNs in the main OE, pheromone detection is mediated by sensory neurons of the VNO, a tube-shaped sensory epithelium that lies within the ventral portion of the nasal septum (Halpern, 1987). Like the main OE, the VNO is derived from the olfactory placode (Farbman, 1992). Although ORN development in the main OE is *Mash1* dependent (Cau et al., 1997), a recent report has suggested that genesis of sensory neurons in the VNO does not require *Mash1* (Cau et al., 2002); however, that study examined only early development (E10.5–12.5). Given that much of the neurogenesis in the VNO is known to occur late during fetal development and in the early postnatal period (for review, see Halpern, 1987), it seemed possible that a requirement for *Mash1* function might not yet be evident in the VNO by E12.5. To resolve this question, we examined the VNO in *Mash1*−/−;*Tattler-4*+/− embryos around the time of birth (E18.5). In wild-type (*Mash1*+/+;*Tattler-4*+/−) animals, the *Tα1:tau-lacZ* transgene is expressed by VNO sensory neurons, and the vomeronasal nerve connecting the VNO to the AOB is heavily labeled by X-gal staining (Fig. 5*A*). However, in *Mash1*−/− animals, the epithelium is much thinner than in wild-type animals, and contains almost no X-gal-stained neurons (Fig. 5*B*). In addition, the size of the vomeronasal nerve is reduced dramatically. These results indicate that most of the sensory neurons of the VNO depend on *Mash1* for their proper development. Moreover, they suggest that the decrease in size of the AOB in *Mash1*−/− animals, shown in Figure 2, is likely to be caused, at least in part, by the loss of sensory afferents from the VNO.

To determine whether other aspects of VNO sensory neuron development show similarities to ORN development in the main OE, we examined the VNO for expression of markers characteristic of different cell stages in the ORN developmental pathway (Fig. 6). ORN development appears to involve three stages of proliferating neuronal progenitor cells, all of which are present in the OE at E14.5–15.5: a neuronal stem cell [defined functionally, because no definitive marker for it has been identified (Mumm et al., 1996)] gives rise to neuronal progenitors that express *Mash1* (Fig. 6*A*) (Gordon et al., 1995). *Mash1*-expressing progenitors then give rise to the immediate neuronal precursors (INPs) of ORNs (Calof and Chikaraishi, 1989). INPs do not express *Mash1*, but instead express *Neurogenin1* (*Ngn1*), another proneural gene homolog encoding a bHLH transcription factor (Fig. 6*B*) (Cau et al., 1997; Calof et al., 1998, 2002; Wu et al., 2003). The progeny of INPs rapidly differentiate into ORNs and express NCAM (Fig. 6*C*) (Calof and Chikaraishi, 1989; DeHamer et al., 1994; Calof et al., 1998). In *Mash1*−/− animals, development of ORNs ceases early in this pathway, and as a consequence expression of the INP- and neuron-specific genes, *Ngn1* and *Ncam*, is drastically reduced in the OE (Fig. 6*E*,*F*) (Cau et al., 1997).

In the VNO at E14.5, *Mash1* is expressed predominantly by

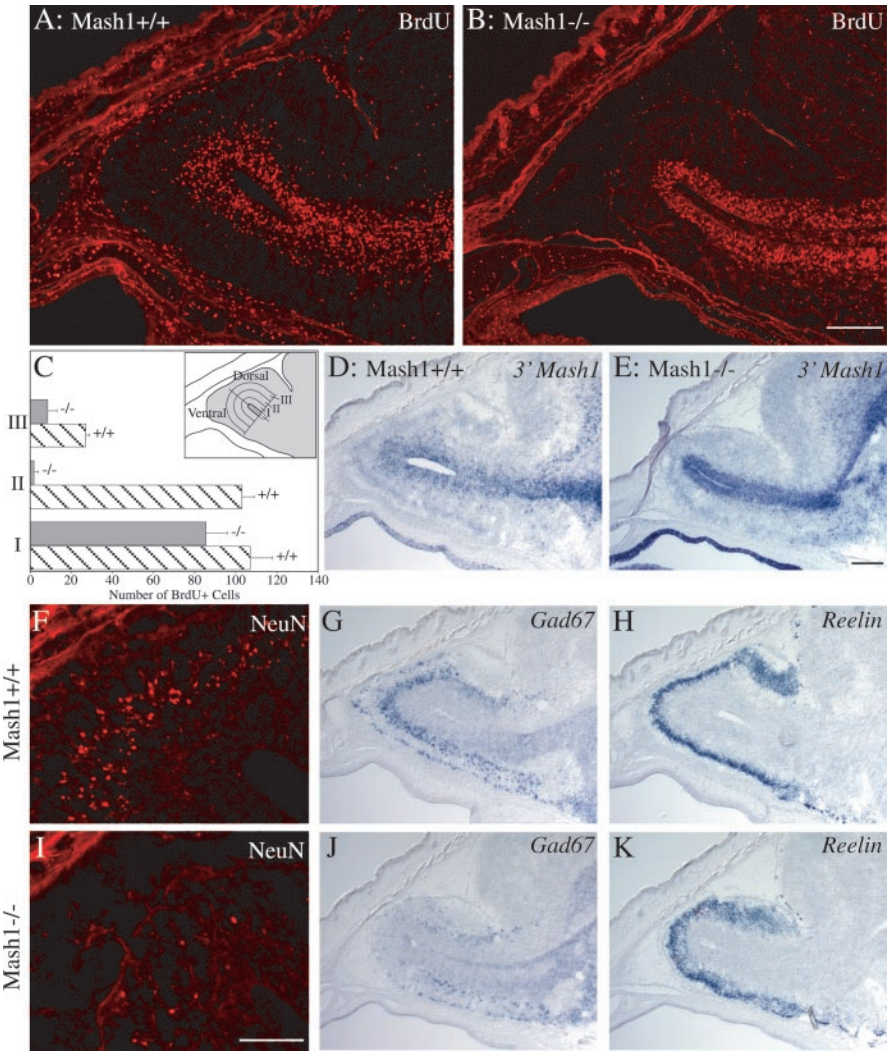

Figure 4. Alterations in RMS, VZ, and granular layer of the OB in *Mash1*−/− embryos. *A*, *B*, *D–K*, Sagittal sections, 12 μm (*A*, *B*, *F*, *I*) and 20 μm (*D*, *E*, *G*, *H*, *J*, *K*), through the heads of E17.5 *Mash1*+/+ embryos (*A*, *D*, *F–H*) and *Mash1*−/− littermates (*B*, *E*, *I–K*) were processed for BrdU or NeuN immunostaining or *in situ* hybridization for 3′ *Mash1* UTR, *Gad67*, or *Reelin* as indicated. Scale bars: (in *B*) *A*, *B*, 200 μm; (in *I*) *F*, *I*, 100 μm; (in *E*) *D*, *E*, *G*, *H*, *J*, *K*, 200 μm. *C*, Quantification of BrdU-incorporating cells in the ventricular zone and granular layer of the OB in *Mash1*−/− embryos (*gray bars*) and wild-type (*striped bars*) littermates. The total number of BrdU+ cells was counted in a series of three 83-μm-wide (approximate width of the ventricular zone) bands proceeding dorsally or ventrally from the OB ventricular surface (*inset*). Values: Band I, 107 (range, ±11) BrdU+ cells (wild type) and 85.5 (range, ±10.5) BrdU+ cells (*Mash1*−/−); Band II, 103 (range, ±6) BrdU+ cells (wild type) and 2 (range, ±2) BrdU+ cells (*Mash1*−/−); Band III, 27 (range, ±2) BrdU+ cells (wild type) and 8.5 (range, +4.5) BrdU+ cells (*Mash1*−/−).

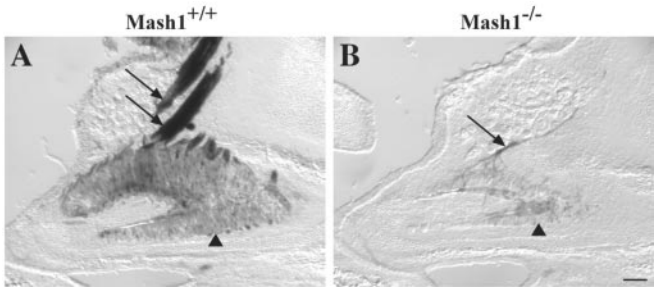

Figure 5. Alterations in the VNO of *Mash1*−/− mice. *A*, *B*, Sagittal sections through the VNO of an E18.5 *Mash1*+/+;*Tattler-4*+/− embryo (*A*) and a *Mash1*−/−;*Tattler-4*+/− littermate (*B*) stained with X-gal. Anterior is on the *left*, and dorsal is at the *top*. *A*, Sensory neurons in the VNO epithelium (*arrowhead*) stain with X-gal as do the vomeronasal nerves (*arrows*). *B*, The number of sensory neurons and the size of the VNO (*arrowhead*) as well as the size of the vomeronasal nerve (*arrow*) is reduced in the *Mash1*−/−;*Tattler-4*+/− littermate. Scale bar, 100 μm.

cells in the basal region, with scattered *Mash1*+ cells located more apically in the epithelium (Fig. 6*G*). This pattern is similar to the pattern of *Mash1* expression in the main OE (Fig. 6*A*) and is consistent with what is known concerning the location of proliferating progenitors in VNO (Weiler et al., 1999). *Ngn1* is also expressed in the basal progenitor cell region of the VNO (Fig. 6*H*), and the neuronal marker *Ncam* is expressed throughout the sensory neuron-containing layers (Fig. 6*I*). To determine whether this is indicative of a developmental hierarchy of gene expression in the VNO sensory neuron lineage similar to that of ORNs in the main OE, we asked whether expression of *Ngn1* and *Ncam* in the VNO is also dependent on *Mash1* function. *Ngn1* is essentially absent in the VNO of *Mash1*−/− embryos at E14.5 (Fig. 6*K*), consistent with the idea that *Ngn1* expression in the VNO is *Mash1*-dependent. In addition, a dramatic reduction in the number of *Ncam*-expressing neurons was also apparent in the VNO of *Mash1*−/− embryos (Fig. 6*L*). By E17.5, near the time of birth, only a few scattered sensory neurons remain in the VNO of *Mash1*−/− animals, as indicated by the decrease of hybridization for probes to either *Ncam* or the VNO neuron-specific channel, *Trp2* (Fig. 6*M-P*) (Liman et al., 1999). Altogether, these findings demonstrate that *Mash1* function is required for the normal development of sensory neurons in the VNO, as it is in the main OE. In addition, they suggest that similar hierarchies of gene expression regulate neuronal differentiation in these two sensory epithelia.

Proliferating neural progenitors are present in the olfactory epithelium and vomeronasal organ of *Mash1*−/− embryos

The failure of sensory neurons to differentiate in the VNO and OE in the absence of *Mash1* function raises questions about the fate of neural progenitor cells in these structures. Because the OE and VNO are thinner and have many fewer neurons in *Mash1*−/− animals (Fig. 6), we hypothesized that progenitor cells might also be absent. To determine whether this was the case, we injected pregnant dams (day 14.5 of gestation) with BrdU and fixed embryos 1 hr later to identify cells in S phase. In wild-type embryos at E14.5, BrdU-labeled cells are located in the basal and apical layers of the OE and in the basal two-thirds of the VNO, regions in which proliferating progenitor cells are known to be located in both of these structures (Fig. 7*A*,*B*) (Smart, 1971; Cuschieri and Bannister, 1975). We also found numerous BrdU+ cells present in both OE and VNO of E14.5 *Mash1*−/− embryos (Fig. 7*C*,*D*). Interestingly, BrdU+ cells in the OE and VNO of *Mash1*−/− embryos are altered in their relative locations within the epithelia compared with wild types. Rather than being localized to the basal and apical compartments of the epithelia, BrdU+ cells are present throughout the apical–basal extent of the epithelia in *Mash1*−/− OE and VNO. In addition, the shape of BrdU-incorporating nuclei differs in embryos of the two genotypes. In *Mash1*−/− animals, the nuclei are larger and spindle-shaped, rather than round or oval in shape, as they are in wild-type embryos (Fig. 7*C*,*D*).

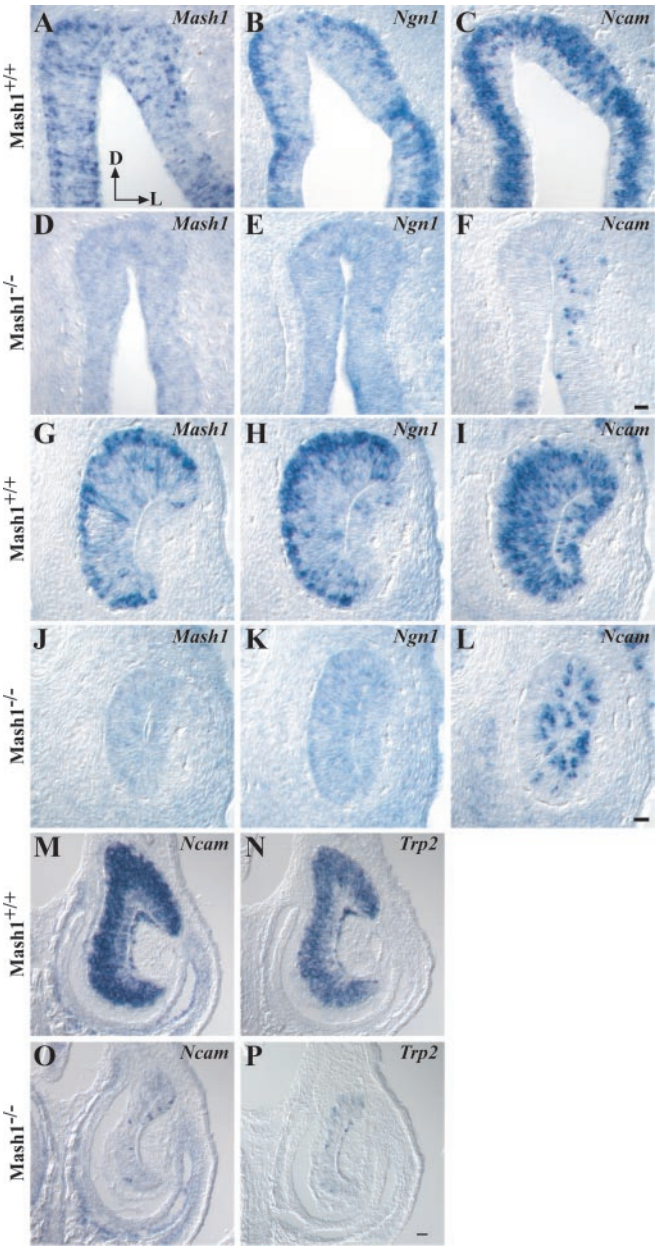

Figure 6. Gene expression in the OE and VNO of *Mash1*−/− embryos. *A–P*, Coronal sections of E14.5 wild-type OE (*A–C*) and VNO (*G–I*) or *Mash1*−/− littermate OE (*D–F*) and VNO (*J–L*) and E17.5 wild-type (*M*, *N*) or *Mash1*−/− littermate VNO (*O*, *P*) were processed for *in situ* hybridization as described in Materials and Methods. Dorsal is at the *top*, and lateral is on the *right* (*A*, *arrows*). Scale bar: (in *F*) *A–F*, 20 μm; (in *L*) *G–L*, 20 μm; (in *P*) *M–P*, 50 μm.

To determine whether the number of proliferating cells is altered in *Mash1*−/− OE and VNO, we performed cell counts in six to eight sections from two animals of each genotype. In wild-type OE, there were 572 (range, ±85) BrdU+ cells per millimeter versus 376 (range, ±2) BrdU+ cells per millimeter OE in

Mash1−/− animals. Because the OE is thinner in *Mash1*−/− mice, we also calculated the density of BrdU+ cells per unit area, and these numbers were very similar: 80 (range, ±25) BrdU+ cells/10,000 μm^2 in wild-type OE versus 81 (range, ±6) BrdU+ cells/10,000 μm^2 in *Mash1*−/− OE. Because the VNO is a circular structure in cross section, it is not possible to accurately count the number of BrdU+ cells per unit length, so only the density of BrdU+ cells per unit area was obtained for this structure: 234 (range, ±5) BrdU+ cells/25,000 μm^2 in wild-type VNO and 201 (range, ±15) BrdU+ cells/25,000 μm^2 in *Mash1*−/− VNO. Thus, the density of proliferating cells is very similar in both the OE and VNO of wild-type and *Mash1*−/− animals.

To determine whether the proliferating cells in the OE and VNO of mutant embryos might be neural progenitors, we used the 3′ *Mash1 in situ* hybridization probe to detect cells expressing mutant *Mash1* transcripts (i.e., presumptive neural progenitors). The pattern of hybridization in the OE and VNO of wild-type embryos observed with this probe was identical to that seen in earlier experiments using a probe containing only the *Mash1* coding region (compare Fig. 7*E*,*F* with Fig. 6*A*,*G*). In *Mash1*−/− embryos, however, the 3′ *Mash1* probe hybridized to the vast majority of cells in OE and VNO, and BrdU-incorporating cells (Fig. 7, compare *G*, *H* with *C*, *D)* were among the expressing cells in both structures. These findings indicate that the proliferating cells present in mutant OE and VNO are capable of expressing *Mash1*, and so in this respect they have at least one characteristic of sensory neuron progenitors. However, these cells fail to express normal *Mash1* or *Ngn1* transcripts, and for the most part they fail to give rise to sensory neurons in either the OE or VNO (Fig. 6) (Guillemot et al., 1993; Gordon et al., 1995; Cau et al., 1997), indicating that they have lost the ability to give rise to neurons.

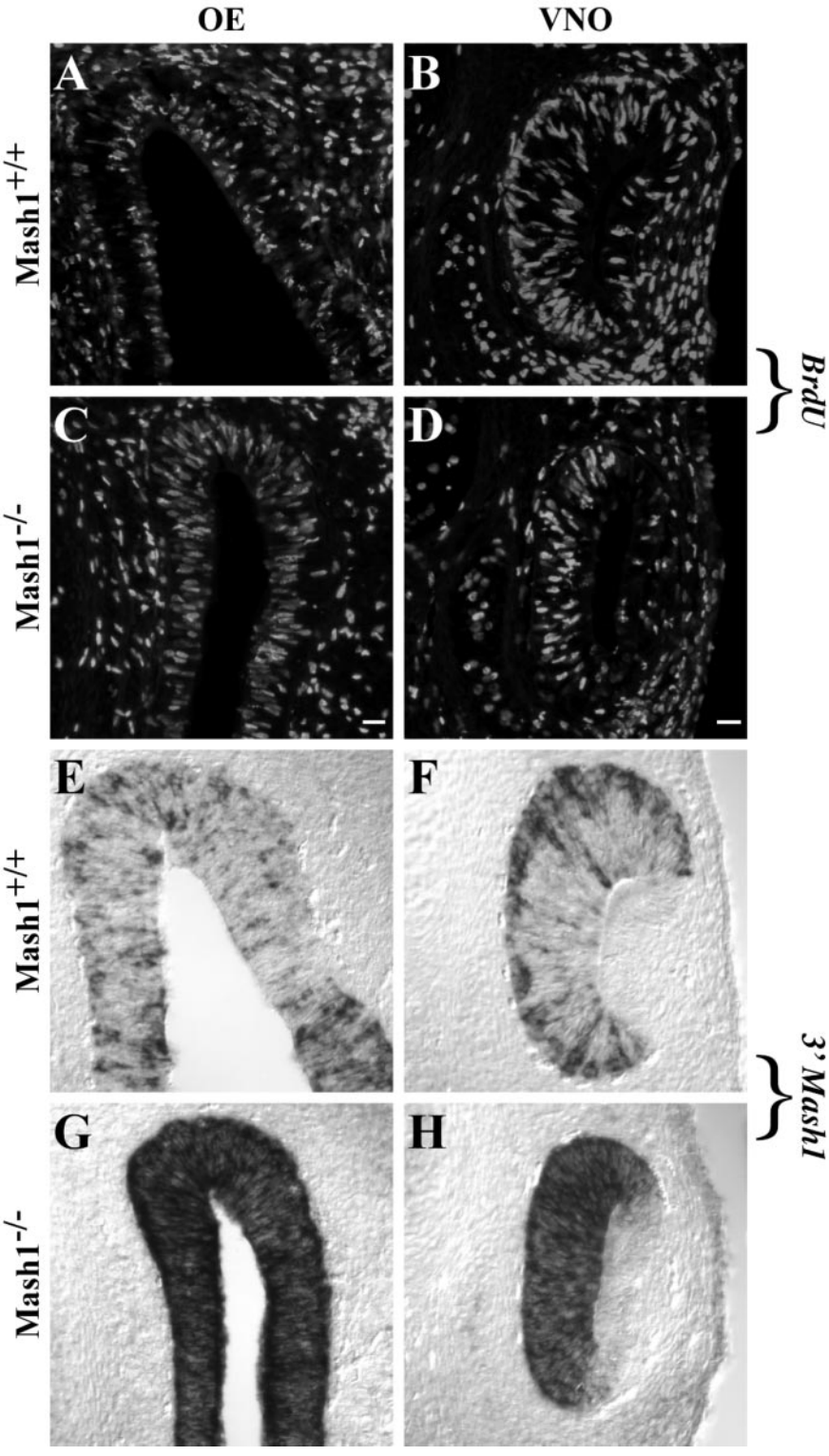

Figure 7. BrdU incorporation and *Mash1* expression in the OE and VNO of *Mash1*−/− embryos. *A–H*, E14.5 wild-type (*A*, *B*, *E*, *F*) and *Mash1*−/− (*C*, *D*, *G*, *H*) littermates were sectioned coronally and processed for BrdU immunohistochemistry (*A–D*) or *in situ* hybridization with the probe for the 3′ *Mash1* UTR (*E–H*). Scale bar: (in *C*) *A*, *C*, *E*, *G*, 20 μm; (in *D*) *B*, *D*, *F*, *H*, 20 μm.

3′ *Mash1*-expressing cells in *Mash1*−/− olfactory epithelium express a sustentacular cell marker

What then is the fate of 3′ *Mash1*-expressing proliferating cells in *Mash1*−/− OE and VNO? To determine whether these cells have characteristics of other cell types in these epithelia, we first used a commercial antiserum to keratins to mark horizontal basal cells (Calof and Chikaraishi, 1989); no difference was observed in the pattern of staining between wild-type and mutant OE and VNO (data not shown). The *Steel* gene has been shown to be expressed by supporting cells (sustentacular cells) of the OE, and a previous study noted that *Steel*-expressing cells are still present in the OE of newborn *Mash1*−/− animals (Guillemot et al., 1993). We generated a *Steel* probe by RT-PCR (see Materials and Methods) and performed *in situ* hybridization experiments on the OE and VNO of E14.5 and E17.5 *Mash1*−/− embryos and wild-type littermates. The results are shown in Figure 8. In wild-type OE at both ages, *Steel* expression is evident in the apical cytoplasm of sustentac-

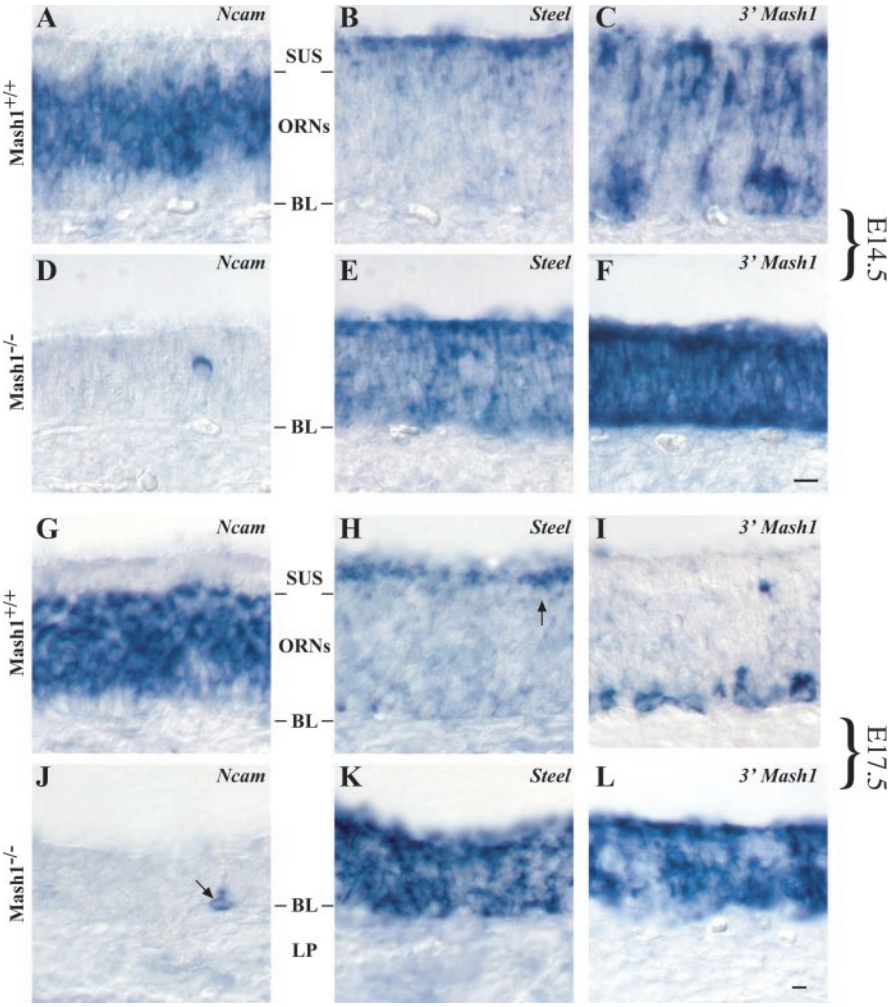

Figure 8. *Ncam*, *Steel*, and 3′ *Mash1* expression in wild-type and *Mash1*−/− embryos. *A–L*, E14.5 (*A–F*) and E17.5 (*G–L*) embryos were sectioned in the coronal plane and processed for *in situ* hybridization. Sustentacular cell layer (*SUS*), olfactory receptor neuron layer (*ORNs*), basal lamina (*BL*), and lamina propria (*LP*) are shown. Scale bar: (in *F*) *A–F*, 10 μm; (in *L*) *G-L*, 10 μm.

ular cells, which are arrayed in a single layer immediately above *Ncam*-expressing ORNs in the epithelium (Fig. 8*A*,*B*,*G*,*H*).In *Mash1*−/− OE, in contrast, *Steel* appears to be expressed by the majority of cells throughout the basal–apical extent of the epithelium, whereas almost no *Ncam*-positive ORNs are present (Fig. 8*D*,*E*,*J*,*K*). (*Steel* is not expressed in either wild-type or *Mash1*−/− VNO; data not shown.) Thus, there appeared to be many more *Steel*-expressing cells in *Mash1*−/− than in wild-type OE, and the position of these cells overlapped with those incorporating BrdU and expressing the 3′ *Mash1* UTR (compare Fig. 7*C* with Fig. 8*E*,*F*,*K*,*L*). To determine the extent of this overlap, we counted the percentage of cells expressing each marker in *Mash1*−/− OE at E14.5: 84.6% (range, ±3.4%) of cells in the mutant OE express *Steel*, and 96% (range, ±0.4%) of cells in mutant OE also label with the 3′ *Mash1* probe, so it must be the case that most of the cells in the mutant OE express both markers. Thus, in the absence of *Mash1* function, the OE becomes populated by proliferating cells that have characteristics of both neuronal progenitors (expression of the 3′ *Mash1* UTR) and supporting (sustentacular) cells (expression of *Steel*).

Increased apoptosis in olfactory epithelium and vomeronasal organ of *Mash1*−/− embryos

Despite the high level of proliferation in *Mash1*−/− OE and VNO (Fig. 7), by the time of birth these epithelia are much thinner than those of wild-type animals (Figs. 2, 5). This observation suggests that the proliferating progenitors present in *Mash1*−/− epithelia do not survive, but instead may be dying at an abnormally high rate. We and others have observed previously that there is an increased level of apoptotic death in cells of *Mash1*−/− OE at E13.5–15.5 (Calof et al., 1996b; Cau et al., 1997). To determine whether cells in *Mash1*−/− VNO also display abnormal levels of apoptosis, we performed TUNEL assays on *Mash1*−/− VNO at E14.5 (Holcomb et al., 1995) (OE was also assessed as a positive control). The results are shown in Figure 9. In wild-type epithelia, almost no TUNEL+ cells can be observed, whereas numerous TUNEL+ cells are present in both OE and VNO of *Mash1*−/− animals. Counting the number of TUNEL+ nuclei confirmed the dramatic increase in the number of apoptotic cells in *Mash1*−/− VNO (e.g., the number of TUNEL+ cells was increased more than fivefold in *Mash1*−/− VNO) (Fig. 9*F*). Thus, despite being able to proliferate and being capable of expressing markers of both neuronal progenitor cells (*Mash1*) and sustentacular cells (*Steel*), many cells in the *Mash1*−/− VNO and OE are unable to survive.

Discussion

Loss of *Mash1* function leads to abnormalities of olfactory bulb progenitors and granule cells

One of the more striking effects in the CNS that we observed in *Mash1*−/− mice was a marked decrease in OB size, evident in both the main OB and the AOB (Fig. 2). Although some reduction in size of the main OB could be expected from the diminished number of ingrowing ORN and VNO axons (Figs. 2, 5), our observations clearly show that much of the reduction occurs in a layer of interneurons, the OB granule cells (Fig. 2*E*). These neurons derive from progenitors that are produced in the subventricular zone of the lateral ventricle, migrate through the RMS into the VZ of the OB, and finally disperse into the OB granule layer.

The fact that *Mash1* is expressed in the VZ of the OB (Fig. 4) (Guillemot and Joyner, 1993; Sommer et al., 1996), as well as the VZ and subventricular zone of the ganglionic eminences (Casarosa et al., 1999; Horton et al., 1999), which contribute cells to the RMS (Wichterle et al., 1999), suggests that loss of *Mash1* function directly affects OB granule neurons and/or their precursors. The alternate possibility—that reduced afferent (ORN) input to the OB in *Mash1*−/− mice indirectly affects granule cell number—is plausible, given data that naris occlusion in early postnatal rodents can cause granule cell apoptosis in the ipsilateral OB (Frazier and Brunjes, 1988; Frazier-Cierpial and Brunjes, 1989; Najbauer and Leon, 1995; Fiske and Brunjes, 2001). However, the time course of deafferentation-induced granule cell apoptosis is likely to be too slow (~10 d) (Petreanu and Alvarez-Buylla, 2002)

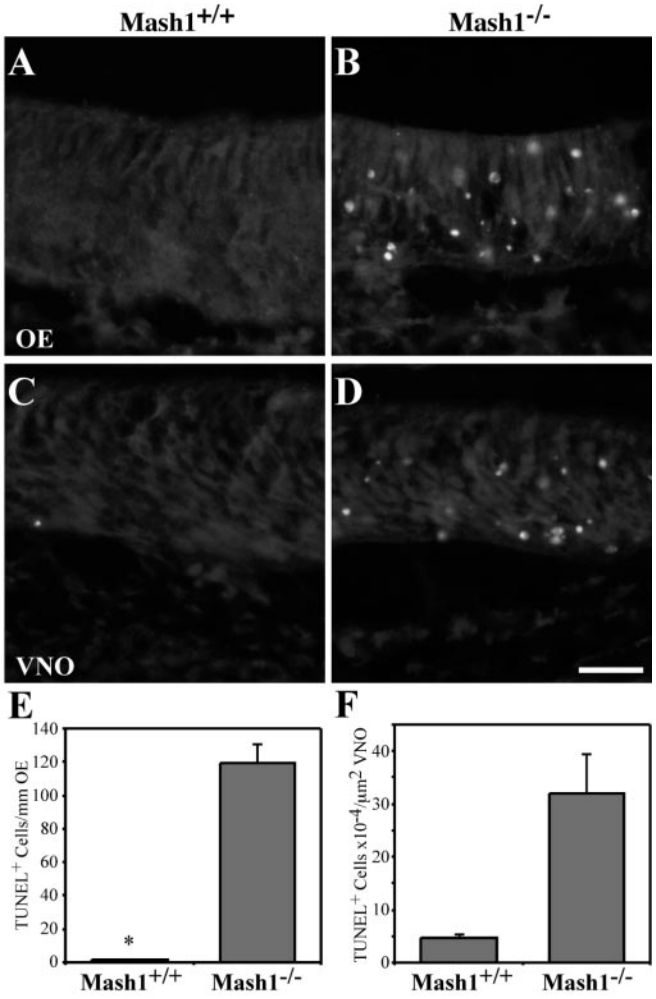

Figure 9. Apoptosis in the OE and VNO of *Mash1*−/− embryos. *A–D*, E14.5 wild-type (*A*, *C*) and *Mash1*−/− (*B*, *D*) littermates were sectioned horizontally at 12 μm and processed for TUNEL labeling as described previously (Holcomb et al., 1995). Scale bar, 20 μm. *E*, The number of TUNEL+ cells per millimeter of OE was counted in a minimum of 20 fields representing at least 5.2 mm of OE in one animal of each genotype. Values are 1.8 (±0.53 SEM) TUNEL+ cells per millimeter OE for wild-type and 119.8 (± 10.87 SEM) TUNEL+ cells per millimeter OE for *Mash1*−/−. *F*, The number of TUNEL+ cells per square micrometers of VNO was counted in a minimum of eight fields representing at least 115,000 μm^2 of VNO. Values are 4.64×10^{-4} (±0.75 SEM) TUNEL+ cells per square micrometer VNO for wild-type and 31.8×10^{-4} (±7.57) TUNEL+ cells per square micrometer VNO for *Mash1*−/−.

to explain the abnormalities in *Mash1*−/− OB at E18.5, just 3–4 d after the initial generation of granule neurons (Hinds, 1968).

Interestingly, in *Mash1*−/−;*Tattler-4*+/− animals, the RMS is noticeably abnormal (Fig. 3*A*,*B*), being both shorter and thicker along the anterior-posterior axis and exhibiting stronger X-gal staining (i.e., increased density of neuronal cells) (Fig. 3*C*,*D*). These changes are reminiscent of mice in which the polysialylated form of NCAM has been rendered nonfunctional by gene inactivation or enzymatic treatment (Cremer et al., 1994; Ono et al., 1994). In such animals, interference with neuronal cell migration into the OB causes an accumulation of cells in the RMS and a reduction in OB size (Bruses and Rutishauser, 2001). If loss of *Mash1* function also results in a migration defect in the RMS, then the fact that *Mash1*−/− animals exhibit normal expression of PSA-NCAM (Fig. 3*E*,*F*) indicates that the cause of this defect would have to be different. It has previously been reported that ventral forebrain neuronal progenitors migrate abnormally in *Mash1*−/− embryos, and this has been linked to premature neuronal differentiation (Horton et al., 1999). The possibility that OB granule neurons also differentiate prematurely is certainly consistent with the observed increased in X-gal staining in the RMS of *Mash1*−/−;*Tattler-4*+/− animals, as the *Tα1:tau-lacZ* transgene is selectively turned on during neuronal differentiation (Fig. 1) (Gloster et al., 1999).

Neurogenesis in the vomeronasal organ: parallels with the olfactory epithelium

Like the main OE, the VNO derives from the olfactory placode, maintains a neuroepithelial structure, projects to the OB, and uses a family of specialized seven-transmembrane odorant receptors to transduce olfactory signals (Halpern, 1987; Dulac, 2000). Despite these similarities, Cau et al. (2002) recently reported only a modest reduction in neuron number in the VNO of *Mash1*−/− animals at E12.5 and concluded that the generation of VNO neurons, unlike those of the main OE, must depend to a large extent on a factor other than *Mash1*. Our observations here support a different view. At E14.5, we observed a substantially reduced number of neurons in the *Mash1*−/− VNO, and by E17.5 a profound reduction was obvious (Fig. 6). These data suggest that although the earliest neurogenesis in the VNO may be *Mash1*-independent, most of the later production of neurons, known to occur late in fetal development and in the early postnatal period (Halpern, 1987), requires *Mash1* function. Interestingly, in the main OE it is also the case that the very earliest generated neurons (those born by E9.5) are relatively *Mash1* independent, whereas those produced later require *Mash1* (Cau et al., 1997). Thus, our results suggest that the molecular details of neurogenesis in the VNO and OE may be more similar than suspected previously. Such a view is supported further by our finding in the E14.5 VNO that *Mash1* is required for expression not just of neuron-specific markers (*Ncam*, *Trp2*), but also of *Ngn1*, a gene that, in the main OE, marks a progenitor cell stage interposed between *Mash1*+ cells and neurons (Cau et al., 1997; Calof et al., 2002).

Do supporting cells and sensory neurons of the olfactory epithelium share a common progenitor?

Despite the deficit in neuron number in the OE and VNO of *Mash1*−/− embryos as early as E14.5 (Fig. 6), we found that many cells in these tissues are proliferating and most express the *Mash1* 3′ UTR (Fig. 7). The observation that the *Mash1* promoter is active in so many more cells in *Mash1*−/− OE and VNO than in wild types suggests that far fewer cells in developing OE and VNO normally express *Mash1* transcripts than are competent to do so. It also supports the findings of Horton and colleagues (1999), whose studies of gene expression in the ventral forebrain of *Mash1*−/− embryos implied that MASH1 negatively regulates its own expression (Horton et al., 1999). Those authors argued that, in *Mash1* nulls, absence of MASH1 protein (required for Notch-Delta signaling) results in a breakdown of the lateral inhibition that is necessary for correct specification of neuronal progenitors from a larger field of competent cells (Lewis, 1996). The idea that *Mash1* functions in the OE through a Notch signaling pathway is supported by the finding that activation of the expression of several genes in this pathway fails to occur in *Mash1*−/− OE (Cau et al., 2000, 2002). Altogether, these observations support a model in which the OE and VNO in *Mash1*−/− embryos are populated by early proliferating progenitor cells that transcribe (aberrant) *Mash1* transcripts, but lacking *Mash1* function, fail to differentiate properly and subsequently undergo apoptosis (Fig. 9).

Interestingly, most (perhaps all) of these presumed early progenitors in *Mash1*−/− OE express *Steel*, a marker of supporting (sustentacular) cells (Fig. 8), together with aberrant *Mash1* transcripts (Figs. 7, 8). This suggests that most of these cells are developing along a sustentacular cell pathway. They also exhibit the elongated nuclei characteristic of sustentacular cells (Fig. 7) (Smart, 1971; Cuschieri and Bannister, 1975). The obvious implication is that, early in embryonic development, the OE may contain bipotential progenitors that subsequently become restricted to a neuronal (ORN) or glial (sustentacular) fate, and that *Mash1* function is required for the neuronal determination event. Indeed, in the inner ear, another placode-derived sensory epithelium, it has been shown that sensory and supporting cells share a common progenitor (Corwin and Cotanche, 1988; Ryals and Rubel, 1988; Fekete et al., 1998). Moreover, in other areas of the nervous system, bHLH transcription factors have been shown to act to promote neuronal, and inhibit glial, fate determination (Tomita et al., 2000; Morrison, 2001; Nieto et al., 2001).

The existence of a common ORN–sustentacular lineage has been suggested by some, but not all, studies. For example, fate maps of single cells in *Xenopus* olfactory placode demonstrated a common progenitor for ORNs and sustentacular cells, at least in early development (Burd et al., 1994). When adult rat OE was lesioned with methyl bromide (which kills both neurons and sustentacular cells) and allowed to regenerate, retroviral lineage mapping suggested the existence of common ORN–sustentacular progenitors (Huard et al., 1998). In contrast, in animals lesioned by olfactory bulbectomy (which kills ORNs but not sustentacular cells), proliferation of cells that express *Mash1* and give rise to neurons increases greatly, but proliferation of cells that become sustentacular cells does not (Gordon et al., 1995; Calof et al., 1996a). Moreover, retroviral lineage analysis of OE in unlesioned postnatal rats failed to find any evidence for a common ORN–sustentacular lineage (Caggiano et al., 1994).

Because sustentacular cells become a self-renewing population shortly after their appearance in the OE, at ~E13.5 (Smart, 1971; Cuschieri and Bannister, 1975; Weiler and Farbman, 1998), one explanation for these data is that the common ORN–sustentacular progenitor generates sustentacular cells only when "needed" to do so. Intriguingly, in the OE there is strong evidence that neuronal production is repressed by feedback signals from ORNs (Mumm et al., 1996; Wu et al., 2003). Perhaps combinations of feedback signals from both ORNs and sustentacular cells cooperatively tell bipotential progenitors not only when to proliferate, but also what cell types to make.

References

Alvarez-Buylla A (1997) Mechanism of migration of olfactory bulb interneurons. Semin Cell Dev Biol 8:207–213.

Angevine Jr JB (1970) Time of neuron origin in the diencephalon of the mouse. An autoradiographic study. J Comp Neurol 139:129–187.

Barthels D, Santoni MJ, Wille W, Ruppert C, Chaix JC, Hirsch MR, Fontecilla-Camps JC, Goridis C (1987) Isolation and nucleotide sequence of mouse NCAM cDNA that codes for a Mr 79,000 polypeptide without a membrane-spanning region. EMBO J 6:907–914.

Blaugrund E, Pham TD, Tennyson VM, Lo L, Sommer L, Anderson DJ, Gershon MD (1996) Distinct subpopulations of enteric neuronal progenitors defined by time of development, sympathoadrenal lineage markers and Mash-1-dependence. Development 122:309–320.

Brunet JF, Ghysen A (1999) Deconstructing cell determination: proneural genes and neuronal identity. BioEssays 21:313–318.

Bruses JL, Rutishauser U (2001) Roles, regulation, and mechanism of polysialic acid function during neural development. Biochimie 83:635–643.

Bulfone A, Wang F, Hevner R, Anderson S, Cutforth T, Chen S, Meneses J, Pedersen R, Axel R, Rubenstein JL (1998) An olfactory sensory map develops in the absence of normal projection neurons or GABAergic interneurons. Neuron 21:1273–1282.

Burd GD, Collazo A, Fraser SE (1994) Cell lineage in the formation and regeneration of the olfactory placodes. Soc Neurosci Abstr 20:1275.

Caggiano M, Kauer JS, Hunter DD (1994) Globose basal cells are neuronal progenitors in the olfactory epithelium: a lineage analysis using a replication-incompetent retrovirus. Neuron 13:339–352.

Callahan CA, Thomas JB (1994) Tau-beta-galactosidase, an axon-targeted fusion protein. Proc Natl Acad Sci USA 91:5972–5976.

Calof AL, Chikaraishi DM (1989) Analysis of neurogenesis in a mammalian neuroepithelium: proliferation and differentiation of an olfactory neuron precursor in vitro. Neuron 3:115–127.

Calof AL, Hagiwara N, Holcomb JD, Mumm JS, Shou J (1996a) Neurogenesis and cell death in olfactory epithelium. J Neurobiol 30:67–81.

Calof AL, Holcomb JD, Mumm JS, Haglwara N, Tran P, Smith KM, Shelton D (1996b) Factors affecting neuronal birth and death in the mammalian olfactory epithelium. Ciba Found Symp 196:188–205.

Calof AL, Mumm JS, Rim PC, Shou J (1998) The neuronal stem cell of the olfactory epithelium. J Neurobiol 36:190–205.

Calof AL, Bonnin A, Crocker C, Kawauchi S, Murray RC, Shou J, Wu H-H (2002) Progenitor cells of the olfactory receptor neuron lineage. Microsc Res Tech 58:176–188.

Casarosa S, Fode C, Guillemot F (1999) Mash1 regulates neurogenesis in the ventral telencephalon. Development 126:525–534.

Cau E, Gradwohl G, Fode C, Guillemot F (1997) Mash1 activates a cascade of bHLH regulators in olfactory neuron progenitors. Development 124:1611–1621.

Cau E, Gradwohl G, Casarosa S, Kageyama R, Guillemot F (2000) Hes genes regulate sequential stages of neurogenesis in the olfactory epithelium. Development 127:2323–2332.

Cau E, Casarosa S, Guillemot F (2002) Mash1 and Ngn1 control distinct steps of determination and differentiation in the olfactory sensory neuron lineage. Development 129:1871–1880.

Chung WW, Lagenaur CF, Yan YM, Lund JS (1991) Developmental expression of neural cell adhesion molecules in the mouse neocortex and olfactory bulb. J Comp Neurol 314:290–305.

Corwin JT, Cotanche DA (1988) Regeneration of sensory hair cells after acoustic trauma. Science 240:1772–1774.

Cremer H, Lange R, Christoph A, Plomann M, Vopper G, Roes J, Brown R, Baldwin S, Kraemer P, Scheff S, Barthels D, Rajewsky K, Wille W (1994) Inactivation of the N-CAM gene in mice results in size reduction of the olfactory bulb and deficits in spatial learning. Nature 367:455–459.

Cuschieri A, Bannister LH (1975) The development of the olfactory mucosa in the mouse: light microscopy. J Anat 119:277–286.

D'Arcangelo G, Miao GG, Chen SC, Soares HD, Morgan JI, Curran T (1995) A protein related to extracellular matrix proteins deleted in the mouse mutant reeler. Nature 374:719–723.

DeHamer MK, Guevara JL, Hannon K, Olwin BB, Calof AL (1994) Genesis of olfactory receptor neurons in vitro: regulation of progenitor cell divisions by fibroblast growth factors. Neuron 13:1083–1097.

Dulac C (2000) Sensory coding of pheromone signals in mammals. Curr Opin Neurobiol 10:511–518.

Farbman AI (1992) Cell biology of olfaction. New York: Cambridge UP.

Fekete DM, Muthukumar S, Karagogeos D (1998) Hair cells and supporting cells share a common progenitor in the avian inner ear. J Neurosci 18:7811–7821.

Fiske BK, Brunjes PC (2001) Cell death in the developing and sensory-deprived rat olfactory bulb. J Comp Neurol 431:311–319.

Fode C, Gradwohl G, Morin X, Dierich A, LeMeur M, Goridis C, Guillemot F (1998) The bHLH protein NEUROGENIN 2 is a determination factor for epibranchial placode-derived sensory neurons. Neuron 20:483–494.

Frazier LL, Brunjes PC (1988) Unilateral odor deprivation: early postnatal changes in olfactory bulb cell density and number. J Comp Neurol 269:355–370.

Frazier-Cierpial L, Brunjes PC (1989) Early postnatal cellular proliferation and survival in the olfactory bulb and rostral migratory stream of normal and unilaterally odor-deprived rats. J Comp Neurol 289:481–492.

Gloster A, Wu W, Speelman A, Weiss S, Causing C, Pozniak C, Reynolds B, Chang E, Toma JG, Miller FD (1994) The T α 1 α-tubulin promoter specifies gene expression as a function of neuronal growth and regeneration in transgenic mice. J Neurosci 14:7319–7330.

Gloster A, El-Bizri H, Bamji SX, Rogers D, Miller FD (1999) Early induction

of Talpha1 alpha-tubulin transcription in neurons of the developing nervous system. J Comp Neurol 405:45–60.
Gordon MK, Mumm JS, Davis RA, Holcomb JD, Calof AL (1995) Dynamics of MASH1 expression in vitro and in vivo suggest a non-stem cell site of MASH1 action in the olfactory receptor neuron lineage. Mol Cell Neurosci 6:363–379.
Guillemot F (1999) Vertebrate bHLH genes and the determination of neuronal fates. Exp Cell Res 253:357–364.
Guillemot F, Joyner AL (1993) Dynamic expression of the murine Achaete-Scute homologue Mash-1 in the developing nervous system. Mech Dev 42:171–185.
Guillemot F, Lo LC, Johnson JE, Auerbach A, Anderson DJ, Joyner AL (1993) Mammalian achaete-scute homolog 1 is required for the early development of olfactory and autonomic neurons. Cell 75:463–476.
Halpern M (1987) The organization and function of the vomeronasal system. Annu Rev Neurosci 10:325–362.
Hatakeyama J, Tomita K, Inoue T, Kageyama R (2001) Roles of homeobox and bHLH genes in specification of a retinal cell type. Development 128:1313–1322.
Hinds JW (1968) Autoradiographic study of histogenesis in the mouse olfactory bulb. I. Time of origin of neurons and neuroglia. J Comp Neurol 134:287–304.
Hogan B (1994) Manipulating the mouse embryo: a laboratory manual, Ed 2. Plainview, NY: Cold Spring Harbor Laboratory.
Holcomb JD, Mumm JS, Calof AL (1995) Apoptosis in the neuronal lineage of the mouse olfactory epithelium: regulation in vivo and in vitro. Dev Biol 172:307–323.
Horton S, Meredith A, Richardson JA, Johnson JE (1999) Correct coordination of neuronal differentiation events in ventral forebrain requires the bHLH factor MASH1. Mol Cell Neurosci 14:355–369.
Huard JM, Youngentob SL, Goldstein BJ, Luskin MB, Schwob JE (1998) Adult olfactory epithelium contains multipotent progenitors that give rise to neurons and non-neural cells. J Comp Neurol 400:469–486.
Jan YN, Jan LY (1994) Genetic control of cell fate specification in *Drosophila* peripheral nervous system. Annu Rev Genet 28:373–393.
Lewis J (1996) Neurogenic genes and vertebrate neurogenesis. Curr Opin Neurobiol 6:3–10.
Liman ER, Corey DP, Dulac C (1999) TRP2: a candidate transduction channel for mammalian pheromone sensory signaling. Proc Natl Acad Sci USA 96:5791–5796.
Lois C, Alvarez-Buylla A (1994) Long-distance neuronal migration in the adult mammalian brain. Science 264:1145–1148.
Luskin MB (1993) Restricted proliferation and migration of postnatally generated neurons derived from the forebrain subventricular zone. Neuron 11:173–189.
Luskin MB (1998) Neuroblasts of the postnatal mammalian forebrain: their phenotype and fate. J Neurobiol 36:221–233.
Ma Q, Kintner C, Anderson DJ (1996) Identification of neurogenin, a vertebrate neuronal determination gene. Cell 87:43–52.
Ma Q, Sommer L, Cserjesi P, Anderson DJ (1997) Mash1 and neurogenin1 expression patterns define complementary domains of neuroepithelium in the developing CNS and are correlated with regions expressing notch ligands. J Neurosci 17:3644–3652.
Ma Q, Chen Z, del Barco Barrantes I, de la Pompa JL, Anderson DJ (1998) Neurogenin1 is essential for the determination of neuronal precursors for proximal cranial sensory ganglia. Neuron 20:469–482.
Marquardt T, Ashery-Padan R, Andrejewski N, Scardigli R, Guillemot F, Gruss P (2001) Pax6 is required for the multipotent state of retinal progenitor cells. Cell 105:43–55.
McConnell JA (1981) Identification of early neurons in the brainstem and spinal cord. II. An autoradiographic study in the mouse. J Comp Neurol 200:273–288.
Morrison SJ (2001) Neuronal differentiation: proneural genes inhibit gliogenesis. Curr Biol 11:R349–351.
Mullen RJ, Buck CR, Smith AM (1992) NeuN, a neuronal specific nuclear protein in vertebrates. Development 116:201–211.
Mumm JS, Shou J, Calof AL (1996) Colony-forming progenitors from mouse olfactory epithelium: evidence for feedback regulation of neuron production. Proc Natl Acad Sci USA 93:11167–11172.
Murray RC, Tapscott SJ, Petersen JW, Calof AL, McCormick MB (2000) A fragment of the Neurogenin1 gene confers regulated expression of a reporter gene in vitro and in vivo. Dev Dyn 218:189–194.
Najbauer J, Leon M (1995) Olfactory experience modulated apoptosis in the developing olfactory bulb. Brain Res 674:245–251.
Nieto M, Schuurmans C, Britz O, Guillemot F (2001) Neural bHLH genes control the neuronal versus glial fate decision in cortical progenitors. Neuron 29:401–413.
Nornes HO, Carry M (1978) Neurogenesis in spinal cord of mouse: an autoradiographic analysis. Brain Res 159:1–6.
Ono K, Tomasiewicz H, Magnuson T, Rutishauser U (1994) N-CAM mutation inhibits tangential neuronal migration and is phenocopied by enzymatic removal of polysialic acid. Neuron 13:595–609.
Petreanu L, Alvarez-Buylla A (2002) Maturation and death of adult-born olfactory bulb granule neurons: role of olfaction. J Neurosci 22:6106–6113.
Pierce ET (1973) Time of origin of neurons in the brain stem of the mouse. Prog Brain Res 40:53–65.
Ryals BM, Rubel EW (1988) Hair cell regeneration after acoustic trauma in adult Coturnix quail. Science 240:1774–1776.
Smart IH (1971) Location and orientation of mitotic figures in the developing mouse olfactory epithelium. J Anat 109:243–251.
Sommer L, Ma Q, Anderson DJ (1996) Neurogenins, a novel family of atonal-related bHLH transcription factors, are putative mammalian neuronal determination genes that reveal progenitor cell heterogeneity in the developing CNS and PNS. Mol Cell Neurosci 8:221–241.
Tomita K, Moriyoshi K, Nakanishi S, Guillemot F, Kageyama R (2000) Mammalian achaete-scute and atonal homologs regulate neuronal versus glial fate determination in the central nervous system. EMBO J 19:5460–5472.
Torii M, Matsuzaki F, Osumi N, Kaibuchi K, Nakamura S, Casarosa S, Guillemot F, Nakafuku M (1999) Transcription factors Mash-1 and Prox-1 delineate early steps in differentiation of neural stem cells in the developing central nervous system. Development 126:443–456.
Tuttle R, Nakagawa Y, Johnson JE, O'Leary DD (1999) Defects in thalamocortical axon pathfinding correlate with altered cell domains in Mash-1-deficient mice. Development 126:1903–1916.
Vannier B, Peyton M, Boulay G, Brown D, Qin N, Jiang M, Zhu X, Birnbaumer L (1999) Mouse trp2, the homologue of the human trpc2 pseudogene, encodes mTrp2, a store depletion-activated capacitative Ca2+ entry channel. Proc Natl Acad Sci USA 96:2060–2064.
Weiler E, Farbman AI (1998) Supporting cell proliferation in the olfactory epithelium decreases postnatally. Glia 22:315–328.
Weiler E, McCulloch MA, Farbman AI (1999) Proliferation in the vomeronasal organ of the rat during postnatal development. Eur J Neurosci 11:700–711.
Wichterle H, Garcia-Verdugo JM, Herrera DG, Alvarez-Buylla A (1999) Young neurons from medial ganglionic eminence disperse in adult and embryonic brain. Nat Neurosci 2:461–466.
Wu H-H, Ivkovic S, Murray RC, Jaramillo S, Lyons KM, Johnson JE, Calof AL (2003) Autoregulation of neurogenesis by GDF11. Neuron 37:197–207.